Icariin attenuates thioacetamide-induced bone loss via the RANKL-p38/ERK-NFAT signaling pathway

LINYAN CHENG[1], XIAOLI JIN[1], HAO SHEN[1], XUANWEI CHEN[1], JIN CHEN[1], BIN XU[2] and JIAN XU[1]

[1]School of Medical Technology and Information Engineering, Zhejiang Chinese Medical University, Hangzhou, Zhejiang 310053; [2]Department of General Surgery, Sir Run Run Shaw Hospital, School of Medicine, Zhejiang University, Hangzhou, Zhejiang 310016, P.R. China

Received October 18, 2021; Accepted January 25, 2022

DOI: 10.3892/mmr.2022.12642

Abstract. There is an increasing incidence of destructive bone disease caused by osteoclast proliferation. This is characterized by reduced bone mass and imbalance of bone homeostasis. Icariin (ICA), a flavonoid compound isolated from *Epimedium*, has anti-osteoporosis activity and inhibits the formation of osteoclasts and bone resorption. The purpose of the present study was to investigate the protective effect of ICA on osteoclastic differentiation induced by thioacetamide (TAA) and its possible mechanism in Sprague Dawley (SD) rats. In the present study, SD rats were intraperitoneally injected with TAA (300 mg/kg) for the bone loss model, treated with ICA (600 mg/kg, intragastric gavage) in the ICA group and TAA+ICA group for treatment of bone loss for 6 weeks. Indexes associated with bone metabolism, such as alkaline phosphatase, N-terminal telopeptide of type-I collagen (NTX-I), calcium (Ca), phosphorus (P) and magnesium (Mg) in the serum, were detected. Osteoclast differentiation of femoral tissues was detected by hematoxylin and eosin and tartrate-resistant acid phosphatase staining. The femoral bone mass was evaluated using a three-point bending test and micro computed tomography. Western blotting was used to detect the expression levels of osteoclast-related proteins in each group. In the rats treated with TAA, the serum concentrations of Ca, P and Mg were decreased, the serum concentration of NTX-I was increased, osteoclast differentiation of the femur was increased, femur bone stress and bone mass were decreased and the bone loss and osteoclast formation were reduced after ICA treatment. In addition, ICA inhibited the protein expression of receptor activator of nuclear factor κ-B ligand (RANKL), receptor activator of nuclear factor κ-B (RANK), p38, ERK, c-Fos and nuclear factor of activated T cells 1 (NFATc1) in the femur of rats treated with TAA. The results suggested that ICA may inhibit osteoclast differentiation by downregulating the RANKL-p38/ERK-NFAT signaling pathway and prevent TAA-induced bone loss. The results are helpful to understand the mechanism of osteoclast differentiation induced by TAA, as well as the antiresorptive activity and molecular mechanism of ICA, and to provide new ideas for the treatment of osteolytic diseases.

Correspondence to: Professor Jian Xu, School of Medical Technology and Information Engineering, Zhejiang Chinese Medical University, 548 Binwen Road, Binjiang, Hangzhou, Zhejiang 310053, P.R. China
E-mail: xujian832002@163.com

Dr Bin Xu, Department of General Surgery, Sir Run Run Shaw Hospital, School of Medicine, Zhejiang University, 3 Qingchun Dong Lu, Shangcheng, Hangzhou, Zhejiang 310016, P.R. China
E-mail: 3304089@zju.edu.cn

Key words: icariin, bone loss, thioacetamide, osteoclast, bone mineral density, nuclear factor of activated T cells

Introduction

Osteoporosis is defined as a progressive bone disease, characterized by low bone mass and deterioration of bone microstructure, resulting in increased brittleness and susceptibility to fracture (1,2). Osteoporosis is caused by an imbalance between bone resorption and bone formation (3) and is a ubiquitous disease that has gradually become a serious public health problem affecting >200 million individuals worldwide (4). Osteoclasts are the only bone tissue cells that can resorb bones and excessive differentiation of osteoclasts can lead to osteolytic diseases, which serve an important role in bone loss in osteoporosis (5). Currently, drugs used for anti-resorption mainly include bisphosphates, calcitonin and selective estrogen receptor modulators (6). However, these drugs have serious side effects, such as osteonecrosis of the jaws and transverse femur fractures, hypercalcemia, hearing loss and breast cancer (7). Therefore, how to effectively prevent and treat bone loss has attracted increasing attention worldwide. Some novel plant-derived drugs deserve to be evaluated in the prevention and treatment of osteoporosis due to their fewer adverse reactions and anti-resorptive activity (4,8,9).

Models of osteoporosis are mainly established through ovariectomy, glucocorticoids induction, low calcium (Ca) diet and disuse osteoporosis. These methods for modeling osteoporosis in animals require complex and long-term effects (10-13). As early as 1984, Lassila (14) reported that thioacetamide (TAA)-induced liver injury is accompanied by changes in serum protein and alveolar bone, mainly manifested in the

reduction of new bone formation. Our previous study established a stable model of bone loss in New Zealand white rabbits via intraperitoneal injection of TAA and it revealed that TAA-induced bone loss mainly promoted osteoclast differentiation (15). Compared with other methods, TAA has the advantages of a short modeling time, being a simple method and high controllability in building a model of bone loss.

Icariin (ICA; $C_{33}H_{40}O_{15}$) is a flavonoid compound extracted from *Epimedium* (16), which has anti-inflammatory, antitumor, anti-depression, anti-oxidation and other biological activities (17,18). Studies have reported that ICA prevents bone loss *in vitro* and restores femoral strength *in vivo* (19,20). ICA can inhibit the osteoclast formation induced by receptor activator of nuclear factor κ-B ligand (RANKL) in RAW264.7 cells (21). Jing *et al (*22). demonstrated that oral ICA treatment prevents bone loss in iron-overloaded mice and inhibited the differentiation and function of osteoclasts. In addition, ICA reduces bone loss induced by methotrexate chemotherapy in rats (23). As these studies demonstrate the osteoporosis-related activity of ICA, it was hypothesized that ICA may exert a protective effect on TAA-induced bone loss.

Although TAA is toxic and carcinogenic to numerous organs, such as the liver, kidney and bone (24,25), it is still widely used in the synthesis of a variety of clinical drugs, chemical materials, pesticides and hair dyes (26,27). In the present study, a TAA-induced bone loss model in rats was established, the protective effect of ICA was explored and the potential mechanisms by which ICA may inhibit osteoclast differentiation were evaluated.

Materials and methods

Reagents and antibodies. TAA (purity >98%) was obtained from Sangon Biotech Co., Ltd. (cat. no. A600940). ICA (purity >98%) was obtained from Xian kai lai Biological Engineering Co., Ltd. (cat. no. I50081). The tartrate-resistant acid phosphatase (TRAP) staining kit (cat. no. 294-67001) was obtained from FUJIFILM Wako Pure Chemical Corporation. RIPA kit (cat. no. P0013B), ECL kit (cat. no. P0018AS), hematoxylin and eosin (H&E; cat. no. C0105) staining kit and acid alcohol slow differentiation solution (cat. no. C0161M) were obtained from Beyotime Institute of Biotechnology. The rat N-terminal telopeptide of type-I collagen (NTX-I) ELISA kit (cat. no. YB-NTXI-Ra) was purchased from Shanghai Yubo Biotechnology Co., Ltd. EDTA decalcified fluid (cat. no. G2520) and the BCA kit (cat. no. PC0020) were obtained from Beijing Solarbio Science & Technology Co., Ltd. The iScript cDNA Synthesis Kit (cat. no. 1708890) and iTaq Universal SYBR Green Supermix (cat. no. 172-5122) were obtained from Bio-Rad Laboratories, Inc. The antibodies against β-actin (cat. no. ab8226), osteopontin (OPN; cat. no. ab73400), TRAP (cat. no. ab191406), cathepsin K (cat. no. ab187647), peroxisome proliferator-activated receptor γ (PPAR-γ; cat. no. ab272718), phosphorylated (p-)JNK (ab76572) and JNK (ab17946) and the secondary antibody (cat. no. ab6721) were purchased from Abcam. The antibodies against IκBα (bs-1287R), p-IκBα (bs-18128R), p65 (bs-23217R), p-p65 (bs-20159R), p38 (cat. no. bs-0637R), ERK (cat. no. bs-0022R), p-p38 (cat. no. bs-0636R) and p-ERK (cat. no. bs-3016R) were obtained from BIOSS. The antibodies against RANKL (cat. no. ABP52325), RANK (cat. no. ABP60088) and c-Fos (cat. no. ABM0065) were purchased from Abbkine Scientific Co., Ltd. The antibody against nuclear factor of activated T cells (NFAT)c1 (cat. no. A1539) was purchased from ABclonal Biotech Co., Ltd. TRIzol® reagent (cat. no. 15596026) was purchased from Thermo Fisher Scientific, Inc. All primers were purchased from Zhejiang Shangya Biotechnology Co., Ltd.

Animals and treatment. A total of 32 specific-pathogen-free grade male Sprague Dawley rats (SD rats; 230-280 g; 8 weeks) were provided by the Shanghai B&K Co. Ltd. The animals were kept at 25˚C and 50±10% humidity with free access to food and water and a 12-h light/dark cycle. After a week of acclimation, all rats were randomly divided into four groups: Rats in the control group were intraperitoneally injected with normal saline as a negative control, rats in the TAA group were intraperitoneally injected with 300 mg/kg TAA, rats in the ICA group were orally treated with 600 mg/kg ICA and rats in the TAA+ICA group were treated with TAA combined with ICA. There were eight rats in each group. The dosages of TAA and ICA were determined based on the results of previous studies and other literature (15,28,29). All rats were treated once every two days for 6 weeks. All animal experiments were performed in accordance with the requirements of the Laboratory Animal-Guideline for ethical review of animal welfare (GB/T 35892-2018) (30).

Blood sample analysis. Blood (0.5 ml) was drawn from the mandibular vein every 2 weeks for blood tests and was collected three times. The serum was obtained by centrifugation (1,500 x g for 15 min at 4˚C). The activity of alkaline phosphatase (ALP), the concentrations of Ca, phosphorus (P) and magnesium (Mg) in the serum were analyzed using a Roche analyzer (Roche Diagnostics). NTX- I levels were detected using an ELISA kit.

H&E and TRAP staining. After fasting for 12 h, the rats were sacrificed by exsanguination under pentobarbital sodium anesthesia (45 mg/kg i.p.) followed by cervical dislocation. All rat femurs were removed and parts of the femurs were placed in 10% neutral formaldehyde for 24 h at room temperature. After 6 weeks of decalcification in EDTA decalcification solution at room temperature, the samples were dehydrated using a gradient of different concentrations of ethanol for 1 h each, washed with xylene and finally embedded in wax. Paraffin sections with a thickness of 4 μm were obtained and stained with H&E and TRAP according to the reagent instructions and pathological changes were observed under an ordinary light microscope (RX50; Ningbo Sunny Instruments Co., Ltd.). The remaining femurs were preserved at -80˚C for subsequent experiments.

Micro computed tomography (CT) analysis. The femur was scanned using a Skyscan1176 μCT scanner (Bruker Belgium SA). The growth plate at the distal end of the rat femur was used as a reference point to move along the sagittal position towards the proximal end and 100 layers were selected as the initial layer and then 100 layers were selected along the sagittal

position towards the proximal end as the region of interest. The image was used to reconstruct the bone microstructure and quantitatively analyze the bone parameters. Parameters for bone mineral density (BMD), ratio of bone volume over tissue volume (BV/TV), trabecular pattern factor (Tb.Pf), trabecular number (Tb.N), the trabecular thickness (Tb.Th) and structure model index (SMI) were directly obtained.

Three-point bending test. The mechanical strength of the femur was measured using a three-point bending test using the Electronic universal testing machine 5569 (Instron) with a span of 15 mm and a loading rate of 5 mm/min. The maximum load and elastic load were calculated according to the load-deformation curve.

Reverse transcription-quantitative PCR. Total RNA was extracted from the femoral head using TRIzol® reagent and quantified by spectrophotometry at 260 nm. The gene amplification instrument 2720 (Applied Biosystems; Thermo Fisher Scientific, Inc.) was used for reverse transcription under the following conditions: 25˚C for 5 min, 46˚C for 20 min and 95˚C for 1 min. A real-time quantitative fluorescence PCR instrument 7500 system (Applied Biosystems; Thermo Fisher Scientific, Inc.) was used for quantitative PCR under the following conditions: Initial denaturation at 95˚C for 30 sec; followed by 40 cycles at 95˚C for 15 sec and 60˚C for 60 sec. qPCR were carried out using iTaq Universal SYBR Green Supermix (Bio-Rad Laboratories, Inc.). RNA extraction, cDNA synthesis and qPCR were performed according to the manufacturer's protocol. GAPDH was used as an internal control. The $2^{-\Delta\Delta Cq}$ method was used to analyze relative gene expression data (31,32). Primer sequences for TRAP, PPAR-γ and GAPDH are shown in Table I.

Western blot analysis. The femoral head samples were ground with liquid nitrogen and then RIPA lysis buffer containing 1 mM PMSF and phosphatase inhibitor was added. The samples were lysed on ice for 30 min, centrifuged at 12,000 x g at 4˚C for 15 min and the supernatant was collected. Protein samples were quantified using a BCA kit. A 10% separation gel and a 5% concentration gel were prepared and 20 μg protein per lane used for electrophoresis and the proteins were transferred onto the PVDF membranes at 4˚C and 200 mA for 2 h at room temperature. PVDF membranes were blocked with 5% skimmed milk in TBS with 0.01% Tween-20 (TBS-T) for 2 h. Subsequently, the PVDF membranes were incubated overnight at 4˚C with primary antibodies against β-actin (dilution, 1:5,000), OPN (dilution, 1:2,000), TRAP (dilution, 1:5,000), cathepsin K (dilution, 1:5,000), PPAR-γ (dilution, 1:1,000), RANK (dilution, 1:1,000), RANKL (dilution, 1:1,000), p38 (dilution, 1:1,000), p-p38 (dilution, 1:1,000), ERK (dilution, 1:1,000), p-ERK (dilution, 1:1,000), JNK (dilution, 1:1,000), p-JNK (dilution, 1:10,000), IκBα (dilution, 1:1,000), p-IκBα (dilution, 1:1,000), p65 (dilution, 1:1,000), p-p65 (dilution, 1:1,000), c-Fos (dilution, 1:1,000) and NFATc1 (dilution, 1:1,000). After three washes with TBS-T, the membranes were incubated with the secondary antibody of IgG (dilution, 1:5,000) for 2 h at room temperature. Finally, the protein bands were visualized using an ECL kit and analyzed using ImageJ 1.8.0 software (National Institutes of Health).

Table I. Primer sequences for reverse transcription-quantitative PCR analysis.

Gene	Sequence (5'-3')	Size, bp
GAPDH		292
Forward	GTGCTGAGTATGTCGTGGAGTCT	
Reverse	ACAGTCTTCTGAGTGGCAGTGA	
TRAP		98
Forward	GTGCATGACGCCAATGACAAG	
Reverse	TTTCCAGCCAGCACGTACCA	
PPAR-γ		271
Forward	CCGAAGAACCATCCGATT	
Reverse	CGGGAAGGACTTTATGTA	

TRAP, tartrate-resistant acid phosphatase; PPAR-γ, peroxisome proliferator-activated receptor γ.

Statistical analysis. Experiments were performed at least three times. Data were analyzed using SPSS 25.0 software (IBM Corp.). All data are presented as the mean ± standard deviation. One-way ANOVA followed by Tukey's post hoc test was performed to compare differences among groups. $P<0.05$ was considered to indicate a statistically significant difference.

Results

ICA inhibits TAA-induced slow growth of SD rats. The growth of rats in each group was observed and recorded. First, the body weight and body length of rats in the TAA group were markedly reduced, the weight changes (weight changes=final weight-initial weight) of the TAA group were markedly reduced compared with the control group and although the weight changes of the TAA + ICA group were also decreased, the weight changes in the TAA + ICA group were increased compared with the TAA group (Fig. 1A and C). The femur of each group was dissected after euthanasia and it was revealed that the femoral length in the TAA group was markedly decreased compared with the control group and the changes were reversed in the TAA + ICA group (Fig. 1B and D).

ICA inhibits the TAA-induced imbalance in serum bone metabolism. In order to observe the effects of ICA and TAA on bone metabolism, the serum levels of ALP, NTX-I, Ca, P and Mg were measured at weeks 2, 4 and 6. Compared with the control group, the activity of ALP in the TAA group was markedly increased at weeks 2, 4 and 6 and these changes were reversed in the TAA + ICA group at week 2 (Fig. 2A). Compared with those of the control group, the levels of NTX-I were markedly increased in the TAA group at week 6 and the NTX-I levels were markedly reduced in the TAA + ICA group compared with the TAA group at week 6 (Fig. 2B). In addition, compared with those in the control group, the serum Ca, P and Mg levels were decreased in the TAA group at weeks 2, 4 and 6 and the TAA + ICA group exhibited a marked recovery at week 6 (Fig. 2C-E).

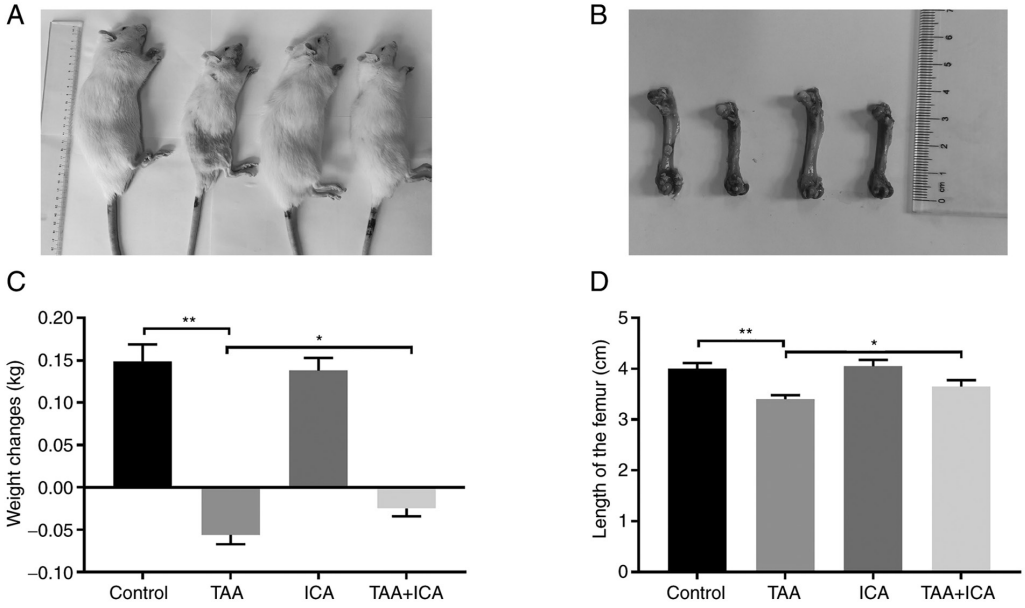

Figure 1. Effects of ICA on the femur and body weight of the SD rats. (A) Morphological images of SD rats in each group. (B) Images of femurs in each group. (C) Effects of ICA on the weight changes. (D) Effects of ICA on the length of the femur. Data are presented as the mean ± SEM of each experiment (n=4). *P<0.05, **P<0.01. ICA, icariin; SD rats, Sprague Dawley rats.

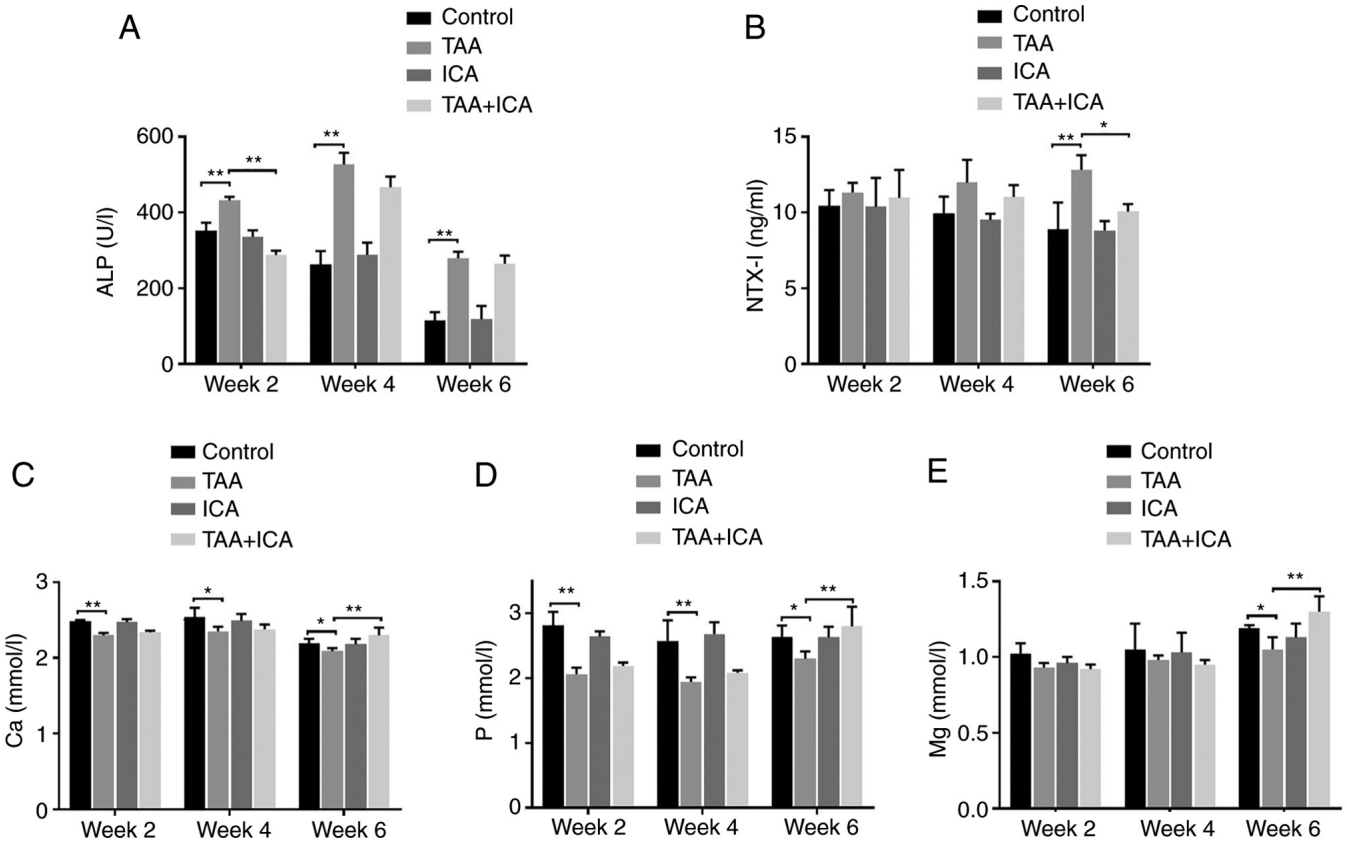

Figure 2. Serum ALP, NTX-I, Ca, P and Mg levels of rats in each group. (A) Serum levels of ALP. (B) Serum levels of NTX-I. (C) Serum levels of Ca. (D) Serum levels of P. (E) Serum levels of Mg. Data are presented as the mean ± SEM of each experiment (n=4). *P<0.05, **P<0.01. ALP, alkaline phosphatase; NTX-I, N-terminal telopeptide of type-I collagen; Ca, calcium; Mg, magnesium; P, phosphorus.

ICA protects against the TAA-induced decrease of the bone trabecular area and osteoclastic differentiation. In order to further understand the effect of ICA on bone tissue injury, pathological analysis of the bone tissue was performed. H&E staining results demonstrated that the structure of the bone trabeculae was disordered and the area of bone trabecula was markedly reduced in the TAA group compared with the control group and these changes were reversed in the TAA + ICA

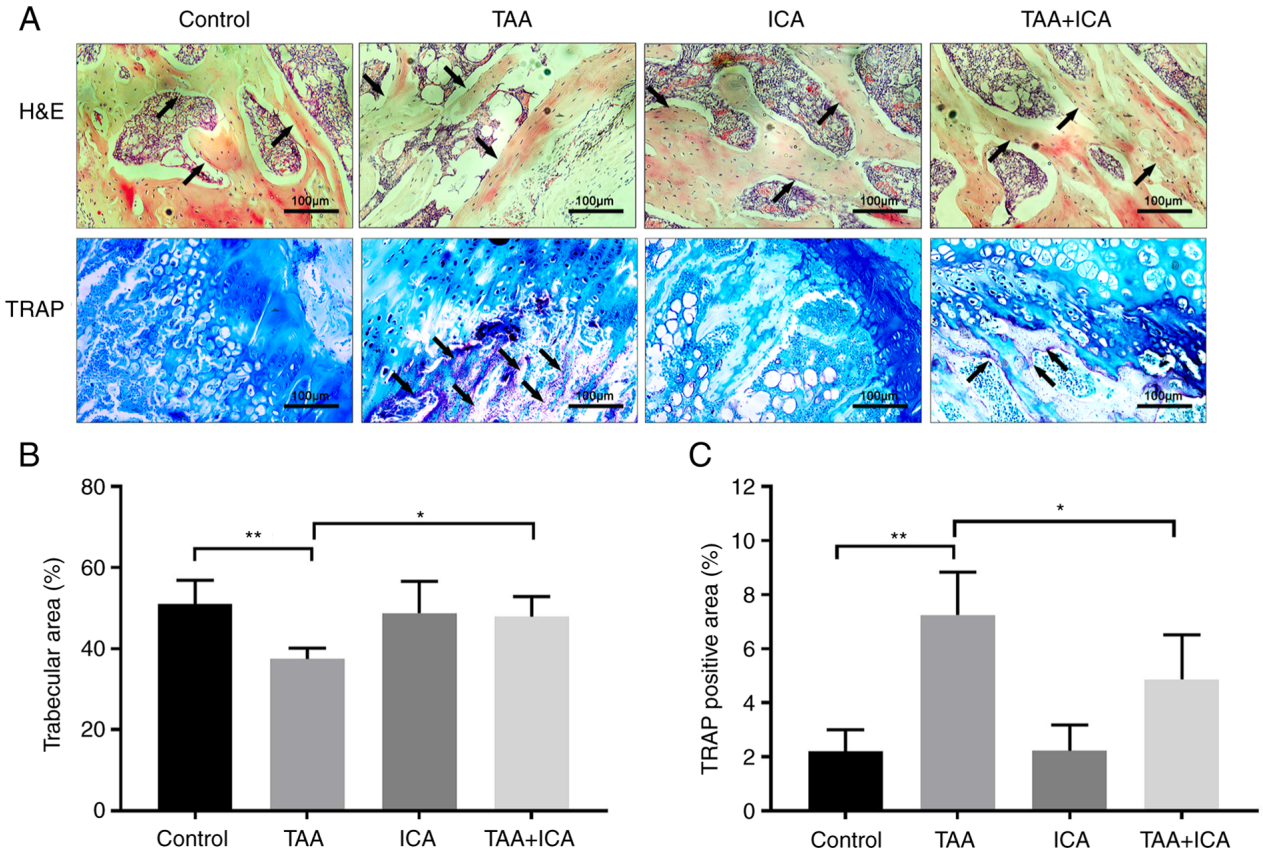

Figure 3. H&E and TRAP staining of femoral tissues in each group. (A) H&E and TRAP staining. Red areas show positive TRAP expression and arrows indicate trabecular bone and TRAP-positive area. (B) Quantitative analysis of the trabecular area of the bone. (C) Quantitative analysis of the TRAP-positive area. The percentage of the trabecular area and the TRAP-positive area was calculated using ImageJ software. Data are presented as the mean ± SEM of each experiment (n=5). Magnification, x200. *P<0.05, **P<0.01. H&E, hematoxylin and eosin; TRAP, tartrate-resistant acid phosphatase.

group (Fig. 3A and B). TRAP staining results revealed that there were obvious red deposits in the TAA group. Compared with those in the TAA group, the positive deposits in the TAA + ICA group were significantly reduced (Fig. 3A and C).

ICA inhibits TAA-induced changes in bone stress. The effect of ICA on the biomechanical strength of TAA rats was analyzed using a three-point bending experiment. The load-deformation curves of each group were obtained using a three-point bending test (Fig. 4A-D). Compared with those of the control group, the elastic modulus and maximum load of the TAA group were markedly reduced (Fig. 4E and F). In addition, compared with that of the TAA group, the elastic modulus of the TAA + ICA group was markedly increased (Fig. 4F).

ICA protects against TAA-induced bone loss. Micro-CT was used to detect the cortical and trabecular microstructures of the femur. In the images obtained using a Micro-CT scan, the number of bone trabeculae, cortical thickness and bone circumference were reduced in the TAA group compared with the control group and those in the TAA + ICA group were improved compared with the TAA group (Fig. 5A). In the cortical bone, BV/TV was markedly reduced in the TAA group compared with the control group and this change was reversed in the TAA + ICA group. In the bone trabeculae, the BMD, BV/TV, Tb.Th and Tb.N of the femur were markedly decreased in the TAA group compared with that in the control group, the Tb.Pf and SMI of the femur were markedly increased in the TAA group compared with that in the control group, and the BMD, Tb.Pf, SMI, Tb.Th and Tb.N were improved in the TAA + ICA group (Fig. 5B).

ICA inhibits TAA-induced expression of osteoclast differentiation-related proteins and genes. To further investigate how ICA affects TAA-induced bone loss, the effects of ICA on bone resorption-related gene and protein expression were examined. The results demonstrated that TAA markedly increased the expression levels of TRAP and PPAR-γ genes, whereas ICA markedly inhibited the expression of these genes (Fig. 6A). The results of western blotting revealed that only the expression levels of osteoclast-related proteins, TRAP and cathepsin K, were significantly different in the TAA group compared with the control group and were decreased in the TAA + ICA group compared with the TAA group, even returning to the levels in the control group. Adipocyte-related protein PPAR-γ and osteoblast-related protein OPN showed no statistical difference among all groups (Fig. 6B).

ICA inhibits TAA-induced expression of RANKL-p38/ERK-NFAT pathway-associated proteins. To explore how ICA affects TAA-induced osteoclast differentiation, the proteins in osteoclast differentiation-related signaling pathways were further examined. Compared with the control group, there was no significant difference in p-JNK and p65

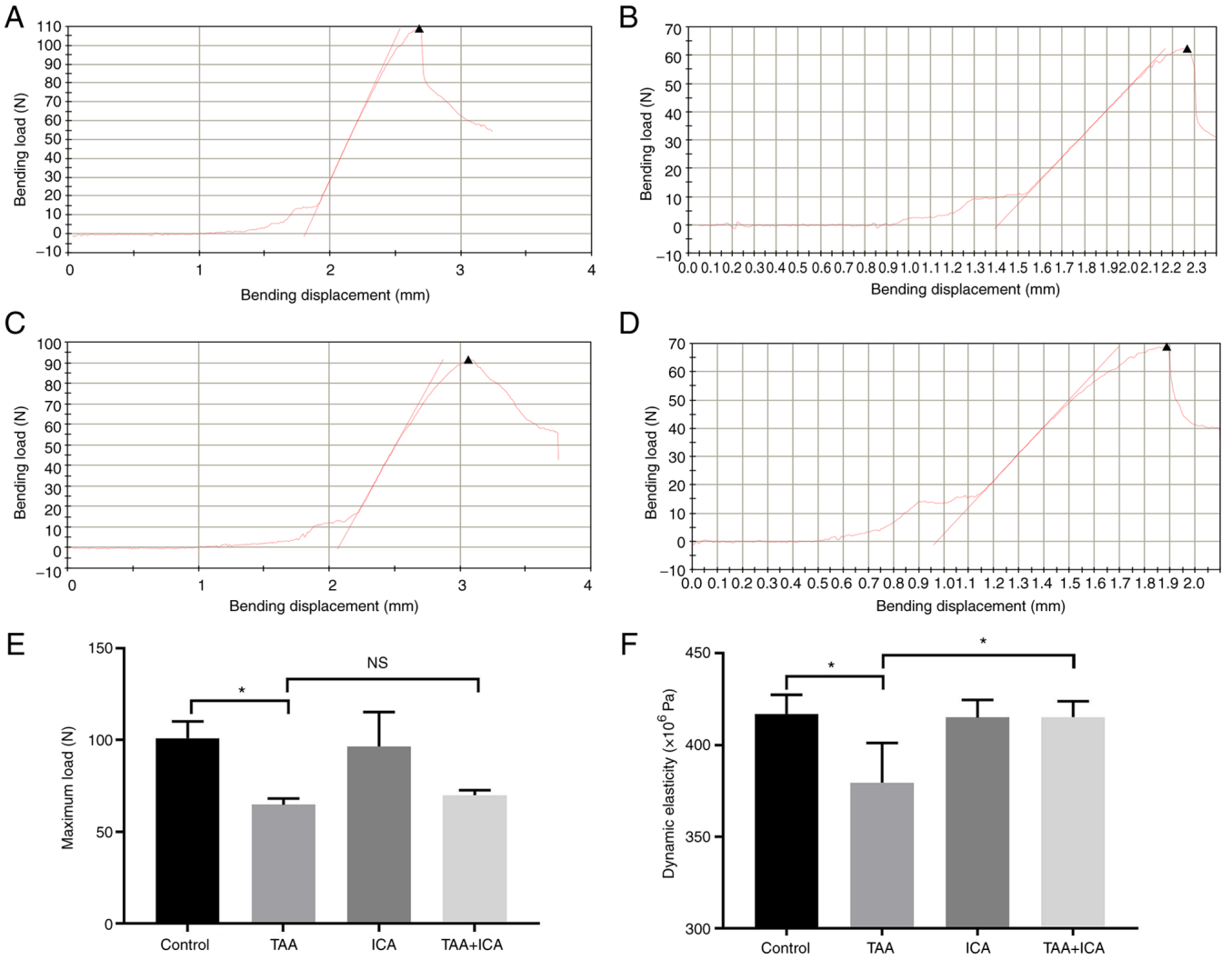

Figure 4. Bone stress in each group as assessed by a three-point bending test. (A-D) Load-deformation curve of the femur in the control, TAA, ICA and TAA + ICA groups. (E) Level of the maximum load. (F) Level of the elastic modulus. '▲' represents the maximum load. Data are presented as the mean ± SEM of three independent experiments for each experiment. *P<0.05. NS, no statistical difference; ICA, icariin; TAA, thioacetamide.

levels in the TAA and TAA + ICA groups and the levels of p-IκBα were increased in the TAA group only. The protein expression levels of RANK, RANKL, p38, ERK, c-Fos and NFATc1 in the TAA group were increased and the protein expression in the TAA + ICA group was inhibited to different degrees compared with the TAA group (Fig. 7).

Discussion

Bone homeostasis is maintained by a balance between osteoclast-induced bone resorption and osteoblast-induced bone formation (33). Destruction of bone remodeling is usually caused by an increase in bone resorption, or a decrease in both bone formation and resorption, resulting in an imbalance of bone homeostasis that leads to bone loss (34). Virtanen *et al* (35) reported that after daily injection of TAA in female rats, the osteoclastic resorption in the alveolar ridge was increased and there was a persistent Ca deficiency in horizontal bone. Furthermore, Nakano *et al* (25) observed that TAA caused hepatic osteodystrophy, which was demonstrated by the reduction of bone volume and bone mass. Therefore, TAA mainly induces osteoporosis by enhancing the activity of osteoclasts and promoting bone resorption. Previous studies have demonstrated that ICA possesses a strong anti-osteoporosis effect and inhibits the differentiation and formation of osteoclasts (36,37). Therefore, in the present study, ICA was used as a drug to inhibit TAA-induced bone loss.

Long-term and short-term weight loss is associated with decreased cortical density, increased cortical porosity and decreased trabecular density and number (38). ICA is beneficial to bone health and can improve bone weight loss, bone length and bone diameter induced by retinoic acid (39). In the present study, ICA inhibited TAA-induced weight loss and the reduction of femoral length in rats. In other words, ICA is beneficial to the normal growth of the body and bone. In addition, when bone loss occurs, the serum ALP concentration increases and the Ca, P and Mg concentrations decrease (40,41). This is consistent with the biochemical results observed following TAA treatment in the present study, where ICA inhibited the TAA-induced increase of serum ALP activity and the decrease of the Ca, P and Mg concentrations. The increased serum ALP activity may be associated with increased bone

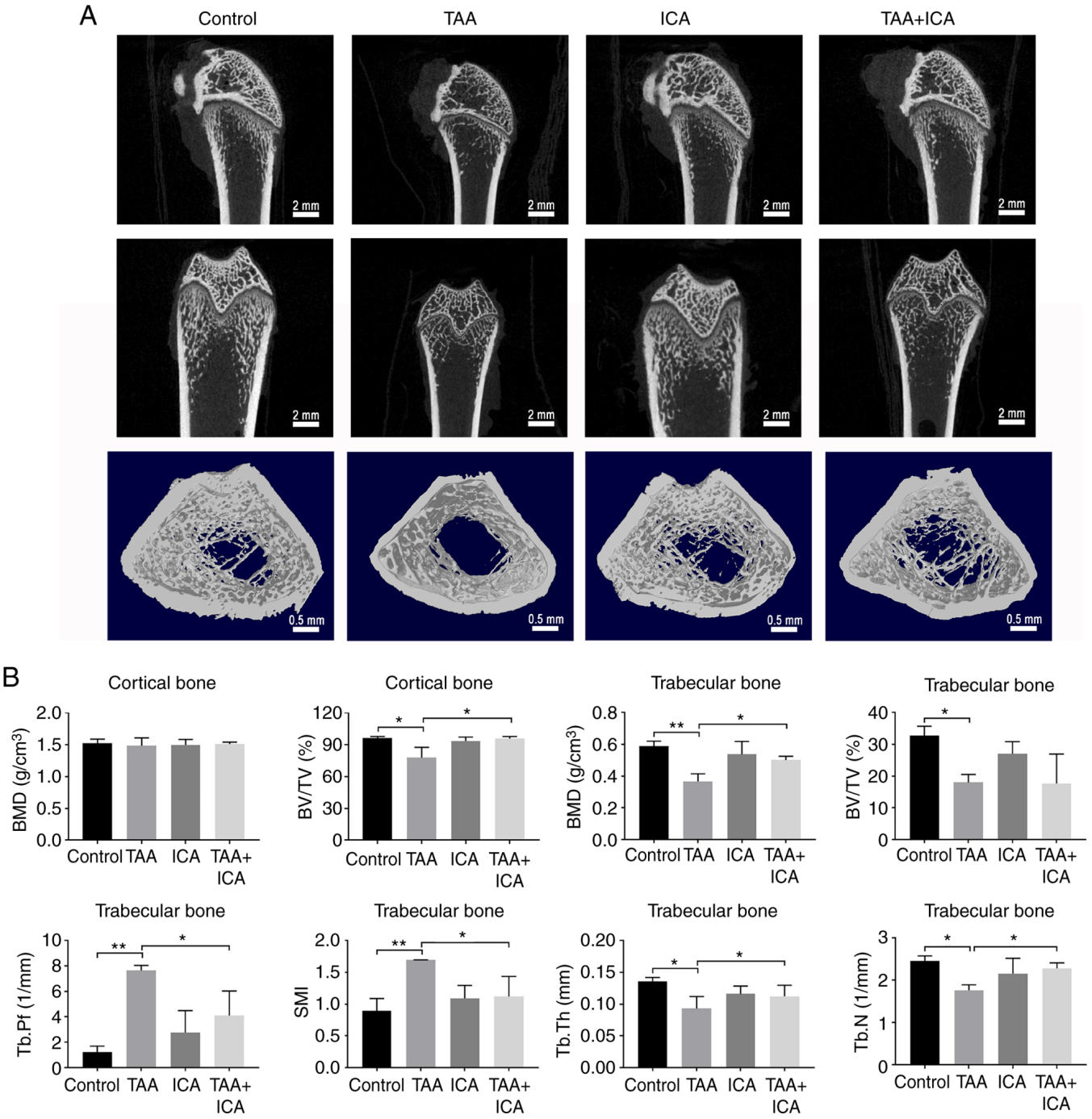

Figure 5. Experimental results of Micro-CT detection of the femur in each group. (A) Scanning images of the Micro-CT. (B) Morphological parameters of the cortical and trabecular bone. Data are presented as the mean ± SEM for three independent experiments in each experiment. *P<0.05, **P<0.01. TAA, thioacetamide; ICA, icariin.

turnover status (42). Osteoclasts release type I collagen and degrade into NTX-I, which is a representative biochemical marker of bone absorption (43). ICA decreased the levels of NTX-I, which were upregulated by TAA and alleviated bone resorption.

Bone mass is low and bone microstructure is damaged in bone loss. BMD or bone mineral content is an important indicator for clinical diagnosis and evaluation of bone loss (44). As a specific marker enzyme for osteoclasts, TRAP can be used as an indicator of the differentiation degree of osteoclasts. There are a large number of TRAP-positive cells in the femur of osteoporotic animals (45). In the present study, the staining results demonstrated that ICA inhibited TAA-induced bone structure disorders, trabecular thinning and the increase of TRAP. At the same time, the three-point bending test and Micro-CT results also revealed that the femur endurance was decreased after TAA treatment and the bone density and other indicators indicated the reduction of bone mass and bone deterioration, especially in the trabecular bone, and ICA could inhibit the TAA-induced bone loss. Similarly, Xu *et al* (46) demonstrate that ICA prevents the loss of alveolar bone and microstructural deterioration caused by estrogen deficiency.

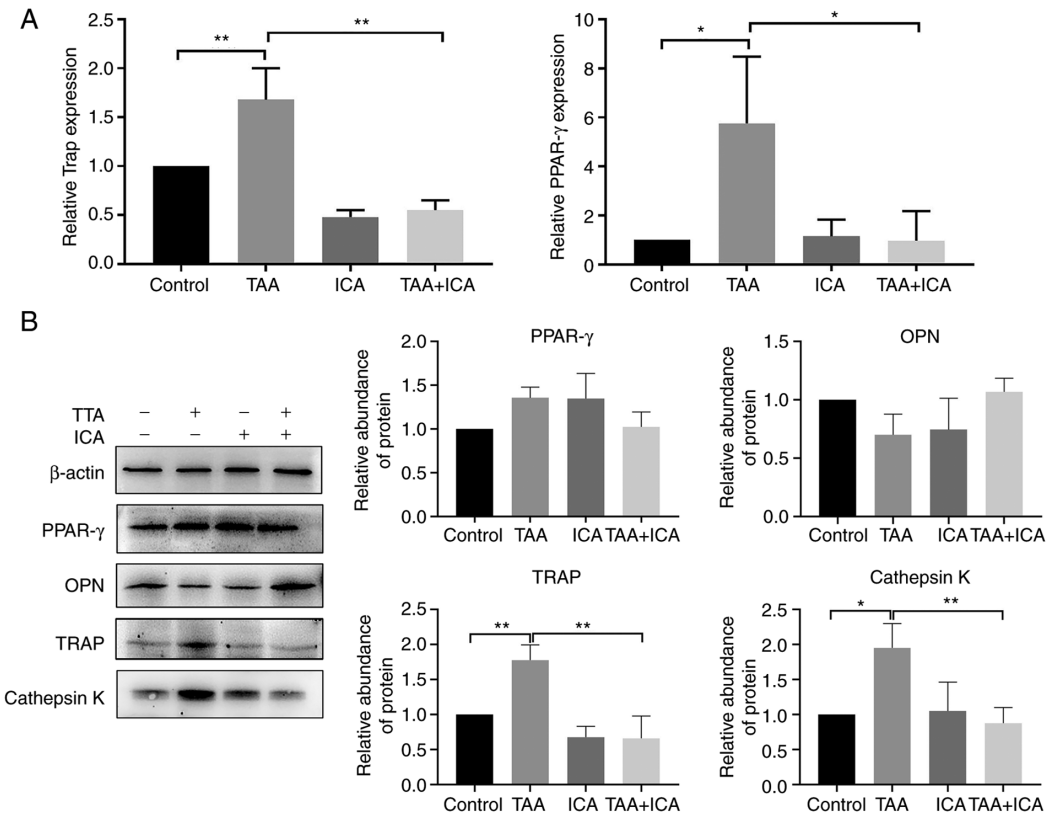

Figure 6. Osteoclast-related proteins and mRNAs in the femoral head of rats in each group. (A) Reverse transcription-quantitative PCR analysis was performed to detect the mRNA expression levels of TRAP and PPAR-γ. (B) Western blotting results for PPAR-γ, OPN, TRAP and cathepsin K proteins. (Left panel) Representative western blot image. (Right panel) Semi-quantitative analysis of protein levels (mean ± SEM; n=3). *P<0.05, **P<0.01. OPN, osteopontin; PPAR-γ, peroxisome proliferator-activated receptor γ; TRAP, tartrate-resistant acid phosphatase.

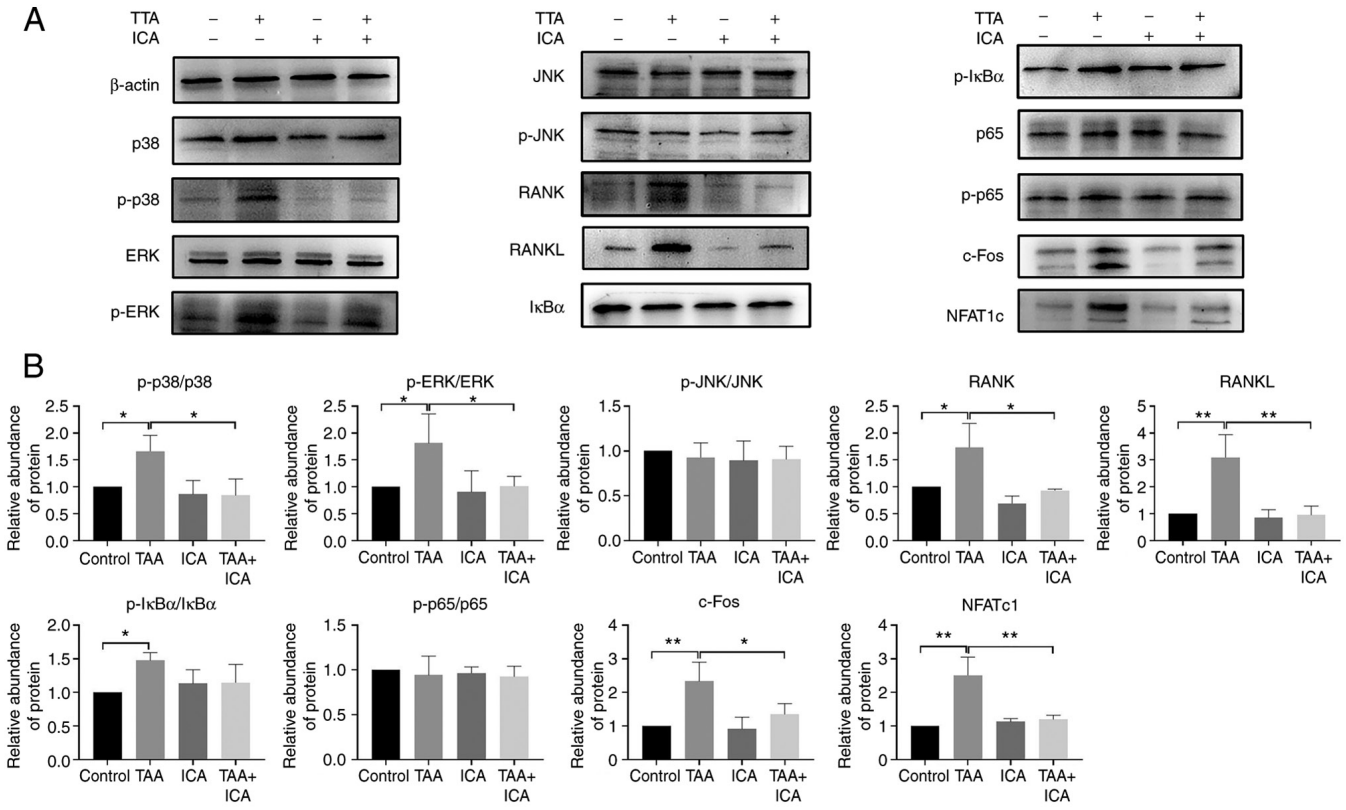

Figure 7. RANKL-p38/ERK-NFAT signaling pathway-associated protein expression in the femur of rats in each group. (A) Western blotting results of protein expression. (B) Relative value of protein expression gray level (mean ± SEM; n=3). *P<0.05, **P<0.01. RANKL, receptor activator of nuclear factor κ-B ligand; NFAT, nuclear factor of activated T-cells; p-, phosphorylated.

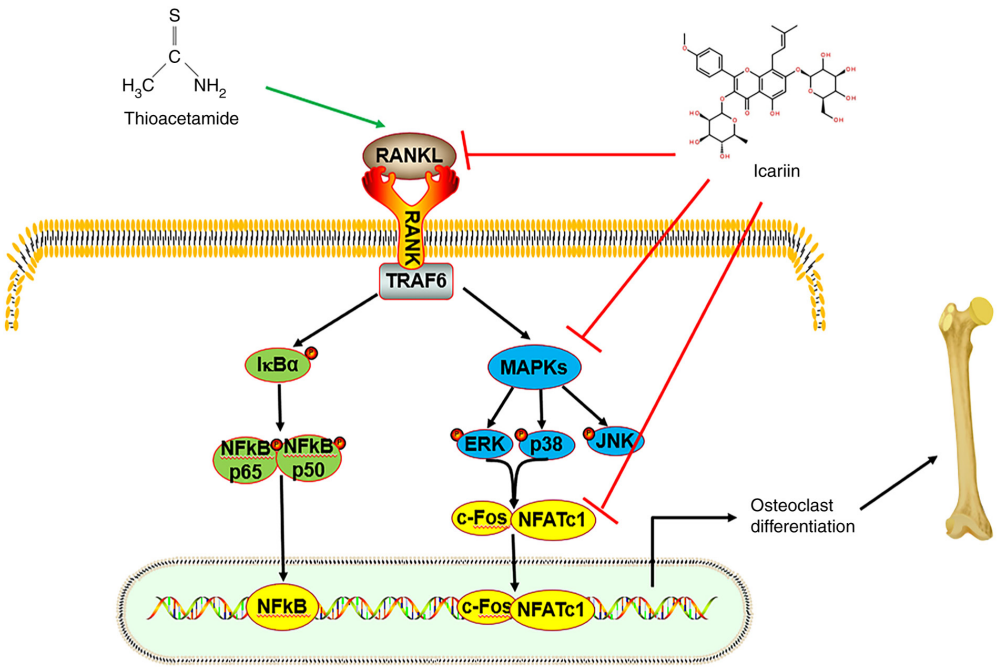

Figure 8. Mechanism of ICA against TAA-induced osteoclast formation. ICA inhibited TAA-induced osteoclast formation by inhibiting activation of RANK and RANKL, phosphorylation of p38 and ERK and transcription of c-Fos and NFATc1. ICA, icariin; NFATc1, nuclear factor of activated T cells 1; RANK, receptor activator of nuclear factor κB; RANKL, receptor activator of nuclear factor κ-B ligand; TAA, thioacetamide.

Huang *et al* (47) revealed that ICA treatment increased trabecular bone density during glucocorticoid exposure. This demonstrates that ICA serves an important role in the improvement of bone structure.

Excessive bone resorption caused by increased osteoclasts is the key to bone loss. In addition, the increase of adipogenic differentiation and the decrease of osteogenic differentiation also lead to the relative increase of osteoclasts, which leads to the increase of bone resorption (36). In order to explore what type of osteocyte differentiation is affected by ICA treatment in bone injury induced by TAA, osteoblast, osteoclast and adipogenesis-related proteins and mRNAs in the femur were detected in the present study. It was revealed that TAA caused bone loss mainly by promoting the expression of osteoclast-related proteins, namely TRAP and cathepsin K, indicating that TAA caused bone loss by promoting osteoclast differentiation.

RANKL binds to RANK on the surface of osteoclast precursor cells to recruit TNF receptor associated factor 6 (TRAF6) and the RANKL-RANK-TRAF6 complex forms and activates NF-κB, MAPKs (ERK, JNK, p38) and NFATc1 signaling pathways to jointly promote osteoclast differentiation and function (48). In the present study, ICA inhibited TAA-induced phosphorylation of p38 and ERK but had no effect on JNK in MAPK kinase. Additionally, ICA inhibited the expression of RANK/RANKL protein induced by TAA and RANKL is a key stimulator of osteoclasts (49), suggesting that ICA and TAA may have antagonistic effects on the binding of RANKL protein. In addition, the activity of p65 was not affected by TAA and ICA did not inhibit the effect of TAA through NF-κB signaling, although the phosphorylation of IκBα was activated. ICA markedly inhibited the expression of c-Fos and NFATc1 induced by TAA. Therefore, ICA downregulated the inhibitory activity of NFATc1 and its anti-TAA-induced osteoclast activity might be mediated via inhibition of the activation of RANKL, P38/ERK and NFATc1 signaling pathways. It has been reported that ICA, the main active component of *Epimedium*, has an anti-osteoporosis effect (50). Feng *et al* (51) demonstrated that ICA activates ERK signaling through estrogen receptor and inhibited glucocorticoid-induced apoptosis of bone cells, demonstrating that ICA may inhibit osteoclast differentiation induced by TAA via the RANKL-p38/ERK-NFAT signaling pathway.

To the best of the authors' knowledge, the bone loss model induced by TAA has not so far been reported. Identifying ICA for the treatment of this model provides ideas for studying the mechanism of bone loss. However, the present study also has some limitations; the molecular pattern of ICA and TAA on the femur and its effect on other bones other than the femur remain to be elucidated. The model of bone injury induced by TAA cannot completely simulate clinical osteoporosis caused by long-term effects. It can mainly be used to quickly establish a bone loss model and provide a warning regarding bone damage in humans exposed to TAA for a long time. In order to further understand the molecular mechanism of TAA-induced bone injury, further cytological experiments will be conducted in the future.

In conclusion, excessive osteoclast differentiation led to an imbalance of bone metabolism, resulting in bone loss and even osteoporosis. Finding effective drugs for bone injury and studying the mechanism of action are of great significance for the prevention, treatment and basic research of diseases. In the current study, the results demonstrated that ICA could improve the bone injury induced by TAA by inhibiting osteoclast differentiation. ICA inhibited TAA-induced osteoclast differentiation by downregulating the RANKL-p38/ERK-NFAT signaling pathway (Fig. 8). The RANKL-p38/ERK-NFAT signaling pathway is a crucial pathway affecting osteoclasts

and its alteration demonstrated the importance of ICA in TAA-induced osteoclast differentiation. These results are helpful for understanding the anti-resorption activity and molecular mechanism of ICA and provide novel ideas for the treatment of destructive bone diseases caused by osteolysis.

Acknowledgements

Not applicable.

Funding

The present study was supported by the Natural Science Foundation of Zhejiang Province (grant no. LY19H060001), the Traditional Chinese Medicine Science and Technology Plan of Zhejiang Province (grant no. 2022ZB093) and the Zhejiang University Student Science and Technology Innovation Activity Plan (grant no. 2020R410056).

Availability of data and materials

The datasets used during the present study are available from the corresponding author upon reasonable request.

Authors' contributions

LC, XJ and HS performed the experiments. LC and HS wrote the manuscript. BX, LC and XC analyzed and interpreted the data. JC and JX contributed to the study design. BX and JX supervised the study and revised the manuscript. LC and JX confirm the authenticity of all the raw data. All authors read and approved the final manuscript.

Ethics approval and consent to participate

The present study was approved by The Animal Ethical and Welfare Committee of Zhejiang Chinese Medical University (approval no. IACUC-20191223-07; Zhejiang, China).

Patient consent for publication

Not applicable.

Competing interests

The authors declare that they have no competing interests.

References

1. Genant HK, Cooper C, Poor G, Reid I, Ehrlich G, Kanis J, Nordin BE, Barrett-Connor E, Black D, Bonjour JP, *et al*: Interim report and recommendations of the world health organization task-force for osteoporosis. Osteoporosis Int 10: 259-264, 1999.
2. Bawa S: The significance of soy protein and soy bioactive compounds in the prophylaxis and treatment of osteoporosis. J Osteoporosis 2010: 891058, 2010.
3. Kenkre JS and Bassett J: The bone remodelling cycle. Ann Clin Biochem 55: 308-327, 2018.
4. Huang YY, Wang ZH, Deng LH, Wang H and Zheng Q: Oral administration of quercetin or its derivatives inhibit bone loss in animal model of osteoporosis. Oxid Med Cell Longev 2020: 1-21, 2020.
5. Tanaka S: RANKL-Independent osteoclastogenesis: A long-standing controversy. J Bone Miner Res 32: 431-433, 2017.
6. Liu Z, Zhang M, Shen Z, Ke J, Zhang D and Yin F: Efficacy and safety of 18 anti-osteoporotic drugs in the treatment of patients with osteoporosis caused by glucocorticoid: A network meta-analysis of randomized controlled trials. PLoS One 15: e0243851, 2020.
7. Looker AC, Johnston CC Jr, Wahner HW, Dunn WL, Calvo MS, Harris TB, Heyse SP and Lindsay RL: Prevalence of low femoral bone density in older U.S. adults from NHANES III. J Bone Miner Res 10: 796-802, 2010.
8. Ma XQ, Han T, Zhang X, Wu JZ, Rahman K, Qin LP and Zheng CJ: Kaempferitrin prevents bone lost in ovariectomized rats. Phytomedicine 22: 1159-1162, 2015.
9. Hwang YH, Ha H, Kim R, Cho CW, Song YR, Hong HD and Kim T: Anti-osteoporotic effects of polysaccharides isolated from persimmon leaves via osteoclastogenesis inhibition. Nutrients 10: 901, 2018.
10. Zhang Z, Zhao Q, Liu T, Zhao H Wang R, Li H, Zhang Y, Shan L, He B, Wang X, *et al*: Effect of Vicenin-2 on ovariectomy-induced osteoporosis in rats. Biomed Pharmacother 129: 110474, 2020.
11. Topolska K, Radzki RP, Filipiak-Florkiewicz A, Florkiewicz A, Leszczyńska T and Cieślik E: Fructan-enriched diet increases bone quality in female growing rats at calcium deficiency. Plant Foods Hum Nutr 73: 172-179, 2018.
12. Wang Y, Chen J, Chen J, Dong C, Yan X, Zhu Z, Lu P, Song Z, Liu H and Chen S: Daphnetin ameliorates glucocorticoid-induced osteoporosis via activation of Wnt/GSK-3β/β-catenin signaling. Toxicol Appl Pharm 409: 115333, 2020.
13. Komori T: Animal models for osteoporosis. Eur J Pharmacol 759: 287-294, 2015.
14. Lassila V and Virtanen P: Influence of experimental liver injury on rat blood and alveolar bone under stress. Acta Anat (Basel) 118: 116-121, 1984.
15. Yao YT, Lu XR, Li Y, Zhou YK, Ren J and Xu J: The new toxic effect of cortical bone osteoporosis induced by thioacetamide. J Toxicol 33: 370-374, 2019.
16. Liang X, Hou Z, Xie Y, Yan F, Li S, Zhu X and Cai L: Icariin promotes osteogenic differentiation of bone marrow stromal cells and prevents bone loss in OVX mice via activating autophagy. J Cell Biochem 120: 13121-13132, 2019.
17. Wang GQ, Li DD, Huang C, Lu DS, Zhang C, Zhou S, Liu J and Zhang F: Icariin reduces dopaminergic neuronal loss and microglia-mediated inflammation in vivo and in vitro. Front Mol Neurosci 10: 441, 2018.
18. Song L, Chen X, Mi L, Liu C, Zhu S, Yang T, Luo X, Zhang Q, Lu H and Liang X: Icariin-induced inhibition of SIRT6/NF-κB triggers redox mediated apoptosis and enhances anti-tumor immunity in triple-negative breast cancer. Cancer Sci 111: 4242-4256, 2020.
19. Nian H, Ma MH, Nian SS and Xu LL: Antiosteoporotic activity of icariin in ovariectomized rats. Phytomedicine 16: 320-326, 2009.
20. Wang J, Tao Y, Ping Z, Zhang W, Hu X, Wang Y, Wang L, Shi J, Wu X, Yang X, *et al*: Icariin attenuates titanium-particle inhibition of bone formation by activating the Wnt/β-catenin signaling pathway in vivo and in vitro. Sci Rep 6: 23827, 2016.
21. Kim B, Lee KY and Park B: Icariin abrogates osteoclast formation through the regulation of the RANKL-mediated TRAF6/NF-κB/ERK signaling pathway in Raw264.7 cells. Phytomedicine 51: 181-190, 2018.
22. Jing X, Du T, Chen K, Guo J, Xiang W, Yao X, Sun K, Ye Y and Guo F: Icariin protects against iron overload-induced bone loss via suppressing oxidative stress. J Cell Physiol 234: 10123-10137, 2019.
23. Hassanshahi M, Su YW, Khabbazi S, Fan CM, Tang Q, Wen X, Fan J, Chen KM and Xian CJ: Icariin attenuates methotrexate chemotherapy-induced bone marrow microvascular damage and bone loss in rats. J Cell Physiol 234: 1-13, 2019.
24. Schyman P, Printz RL, Estes SK, Boyd KL, Shiota M and Wallqvist A: Identification of the toxicity pathways associated with thioacetamide-induced injuries in rat liver and kidney. Front Pharmacol 9: 1272, 2018.
25. Nakano A, Kanda T and Abe H: Bone changes and mineral metabolism disorders in rats with experimental liver cirrhosis. J Gastroenterol Hepatol 11: 1143-1154, 1997.
26. El-Shwiniy WH and Sadeek SA: Synthesis and characterization of new 2-cyano-2-(p-tolyl-hydrazono)-thioacetamide metal complexes and a study on their antimicrobial activities. Spectrochimica Acta A Mol Biomol Spectrosc 137: 535-546, 2014.

27. Gao M, Wang M and Zheng QH: Synthesis of carbon-11-labeled imidazopyridine- and purine-thioacetamide derivatives as new potential PET tracers for imaging of nucleotide pyrophosphatase/phosphodiesterase 1 (NPP1). Bioorg Med Chem Lett 26: 1371-1375, 2016.
28. Khattab A, Hassanin L and Zaki N: Self-nanoemulsifying drug delivery system of coenzyme (Q10) with improved dissolution, bioavailability, and protective efficiency on liver fibrosis. AAPS PharmSciTech 18: 1657-1672, 2016.
29. Zhang Y, Han B, Wei Y, Jing J and Li J: Icariin promotes fracture healing in ovariectomized rats. Med Sci Monit 26: e924554, 2020.
30. Clark JA and Sun D: Guidelines for the ethical review of laboratory animal welfare People's Republic of China National Standard GB/T 35892-2018 [Issued 6 February 2018 Effective from 1 September 2018]. Animal Model Exp Med 3: 103-113, 2020.
31. Zeng Q, Lu W, Deng Z, Wu J and Xu X: Tablysin-15 inhibits osteoclastogenesis and LPS-induced bone loss via attenuating the integrin αvβ3 pathway. Chem Biol Interact 327: 109179, 2020.
32. Livak KJ and Schmittgen TD: Analysis of relative gene expression data using real-time quantitative PCR and the 2(-Delta Delta C(T)) method. Methods 25: 402-408, 2001.
33. Chen Z, Irie N, Takada Y, Shimoda K, Miyamoto T, Nishiwaki T, Suda T and Matsuo K: Bidirectional ephrinB2-EphB4 signaling controls bone homeostasis. Cell Metabolism 4: 111-121, 2006.
34. Armas LA and Recker RR: Pathophysiology of osteoporosis: New mechanistic insights. Endocrinol Metab Clin North Am 41: 475-486, 2012.
35. Virtanen P and Lassila V: Influence of thioacetamide-provoked liver injury on female rat blood and alveolar bone under stress. Acta Anat (Basel) 127: 285-289, 1986.
36. Qi S, He J, Zheng H, Chen C and Lan S: Icariin prevents diabetes-induced bone loss in rats by reducing blood glucose and suppressing bone turnover. Molecules 24: 1871, 2019.
37. Cui J, Zhu M, Zhu S, Wang G, Xu Y and Geng D: Inhibitory effect of icariin on Ti-induced inflammatory osteoclastogenesis. J Surg Res 192: 447-453, 2014.
38. Liu CT, Shivani S, Xu H, McLean RR, Broe KE, Hannan MT, Boyd SK, Bouxsein ML, Kiel DP and Samelson EJ: Long-term and recent weight change are associated with reduced peripheral bone density, deficits in bone microarchitecture, and decreased bone strength: The framingham osteoporosis study. J Bone Miner Res 33: 1851-1858, 2018.
39. Oršolić N, Nemrava J, Jeleč Ž, Kukolj M, Odeh D, Terzić S, Fureš R, Bagatin T and Bagatin D: The beneficial effect of proanthocyanidins and icariin on biochemical markers of bone turnover in rats. Int J Mol Sci 19: 2746, 2018.
40. Zhang J, Fu Q, Ren Z, Wang Y, Wang C, Shen T, Wang G and Wu L: Changes of serum cytokines-related Th1/Th2/Th17 concentration in patients with postmenopausal osteoporosis. Gynecol Endocrinol 31: 183-190, 2014.
41. Yang W, Zhang Y, Yang J, Tan L and Yang K: Potential anti-osteoporosis effect of biodegradable magnesium implanted in STZ-induced diabetic rats. J Biomed Mater Res A 99: 386-394, 2011.
42. Jing Z, Wang C, Yang Q, Wei X, Jin Y, Meng Q, Liu Q, Liu Z, Ma X, Liu K, *et al*: Luteolin attenuates glucocorticoid-induced osteoporosis by regulatingERK/Lrp-5/GSK-3β signaling pathway in vivo and in vitro. J Cell Physiol 234: 4472-4490, 2019.
43. Dénarié D, Constant E, Thomas T and Marotte H: Could biomarkers of bone, cartilage or synovium turnover be used for relapse prediction in rheumatoid arthritis patients? Mediators Inflamm 2014: 537324, 2014.
44. Feng M, Zhang RR, Gong F, Yang P, Fan L, Ni J, Bi W, Zhang Y, Wang C and Wang K: Protective effects of necrostatin-1 on glucocorticoid-induced osteoporosis in rats. J Steroid Biochem Mol Biol 144: 455-462, 2014.
45. Liu X, Fan JB, Hu J, Li F, Yi R, Tan F and Zhao X: Lactobacillus Fermentum ZS40 prevents secondary osteoporosis in wistar rat. Food Sci Nutr 8: 5182-5191,2020.
46. Xu H, Zhou S, Qu R, Yang Y, Gong X, Hong Y, Jin A, Huang X, Dai Q and Jiang L: Icariin prevents oestrogen deficiency-induced alveolar bone loss through promoting osteogenesis via STAT3. Cell Prolif 53: e12743, 2020.
47. Huang M, Wang Y and Peng R: Icariin alleviates glucocorticoid-induced osteoporosis through EphB4/Ephrin-B2 axis. Evid Based Complement Alternat Med 2020: 2982480, 2020.
48. Guo J, Ren R, Sun K, Yao X, Lin J, Wang G, Guo Z, Xu T and Guo F: PERK controls bone homeostasis through the regulation of osteoclast differentiation and function. Cell Death Dis 11: 847, 2020.
49. Boyce BF: Advances in the regulation of osteoclasts and osteoclast functions. J Dent Res 92: 860-867, 2013.
50. Chen KM, Ge BF, Liu XY, Ma PH, Lu MB, Bai MH and Wang Y: Icariin inhibits the osteoclast formation induced by RANKL and macrophage-colony stimulating factor in mouse bone marrow culture. Pharmazie 62: 388-391, 2007.
51. Feng R, Feng L, Yuan Z, Wang D, Wang F, Tan B, Han S, Li T, Li D and Han Y: Icariin protects against glucocorticoid-induced osteoporosis in vitro and prevents glucocorticoid-induced osteocyte apoptosis in vivo. Cell Biochem Biophys 67: 189-197, 2013.